Verification of gyrokinetic δf simulations of electron temperature gradient turbulence

W. M. Nevins
Lawrence Livermore National Laboratory, Livermore, California 94551, USA

S. E. Parker and Y. Chen
University of Colorado, Boulder, Colorado 80309, USA

J. Candy
General Atomics, San Diego, California 92186, USA

A. Dimits
Lawrence Livermore National Laboratory, Livermore, California 94551, USA

W. Dorland
University of Maryland, College Park, Maryland 20742, USA

G. W. Hammett
Princeton Plasma Physics Laboratory, Princeton, New Jersey 08536, USA

F. Jenko
Max-Planck Institut für Plasmaphysik, D-85748 Garching, Germany

The GEM gyrokinetic δf simulation code [Y. Chen and S. Parker, J. Comput. Phys. **189**, 463 (2003); **220**, 839 (2007)] is shown to reproduce electron temperature gradient turbulence at the benchmark operating point established in previous work [W. M. Nevins, J. Candy, S. Cowley, T. Dannert, A. Dimits, W. Dorland, C. Estrada-Mila, G. W. Hammett, F. Jenko, M. J. Pueschel, and D. E. Shumaker, Phys. Plasmas **13**, 122306 (2006)]. The electron thermal transport is within 10% of the expected value, while the turbulent fluctuation spectrum is shown to have the expected intensity and two-point correlation function. © *2007 American Institute of Physics.*
[DOI: 10.1063/1.2759890]

There has been much recent work on computer simulations of electron temperature gradient (ETG) turbulence.[1–13] The differences among these simulations raised questions regarding the reliability of the gyrokinetic simulation codes employed by various workers. An explanation for some of the differences was presented in Ref. 12, and the issue was addressed more broadly in Ref. 14 by demonstrating that the GYRO,[15] GS2,[2] GENE,[1] and PG3EQ[16] codes get substantially the same result when simulating ETG turbulence at the same operating point and with similar numerical resolution. The purpose of this Brief Communication is to demonstrate that the GEM code yields substantially the same results at this ETG benchmark operating point as those obtained by GYRO, GS2, GENE, and PG3EQ. In light of the recent differences in electron energy transport reported for ETG turbulence, verification of these widely used turbulence simulation codes is a critical first step toward using these codes as tools for understanding anomalous transport in tokamak plasmas.

GEM is a global gyrokinetic turbulence simulation code employing the δf particle-in-cell method.[17] GEM uses realistic equilibrium profiles and arbitrary axisymmetric magnetic equilibria.[18] Electrons can be either drift-kinetic, gyrokinetic or adiabatic and ions are either gyrokinetic or adiabatic. GEM can include perpendicular magnetic perturbations (electromagnetic), electron-ion collisions, equilib-

rium shear flow, and minority species ions. However, the simulations of ETG turbulence reported here retain only the electrostatic fields. The electrons are gyrokinetic and the ions are assumed to be adiabatic.[13] These GEM simulations were run on the Cray XT3 at the National Center for Computational Sciences, Oak Ridge National Laboratory.

The ETG benchmark operating point is a variation on the CYCLONE ITG benchmark[19,20] in which the role of electrons and ions have been interchanged, the field-solve modified such that ions provide Debye shielding to the total potential (rather than just shielding the deviation from the flux-surface average of the potential), and the magnetic shear, $s=(r/q)dq/dr$, is reduced from $s=0.79$ to $s=0.1$. Simulations were performed in a flux tube with a radial dimension $L_x=100\rho_e$ and a binormal dimension $L_y=64\rho_e$ (the binormal direction is within a flux surface and perpendicular to $\boldsymbol{B}$) with radial and binormal resolution out to $k_{max}\rho_e=0.82$. The GEM simulations reported here used 128 grid points in the radial direction, 64 grid points in the binormal, and a time step $dt=0.74L_T/v_{te}$. The number of grid cells parallel to the magnetic field was 32, and there were a total of 33 554 432 particles or 128 particles per grid cell.

The quantity of most importance is the electron thermal conductivity which results from the ETG turbulence, $\chi_e \equiv -\langle Q_e \rangle / n_{e0} \nabla T_{e0}$, where $\langle Q_e \rangle$ is the flux-tube averaged electron heat flux, n_{e0} is the equilibrium electron density, and
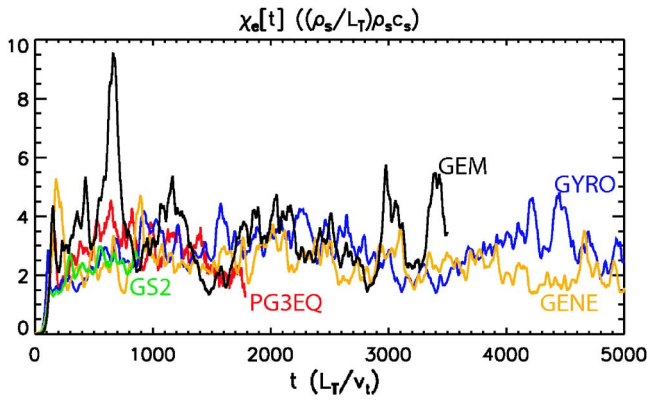
FIG. 1. (Color online) The electron thermal conductivity from GEM (black curve) is compared to results from PG3EQ (red curve), GYRO (blue curve), GS2 (green curve), and GENE (yellow curve).
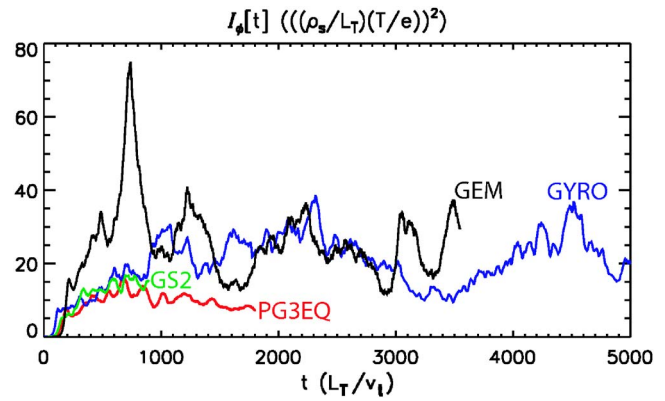

FIG. 2. (Color online) The intensity of the ETG turbulence from GEM (black curve) is compared to that from PG3EQ (red curve), GYRO (blue curve), and GS2 (green curve).

∇T_{e0} is the equilibrium electron temperature gradient. In Fig. 1 the electron thermal conductivity in our GEM simulations is compared to the electron thermal conductivities reported in Ref. 14 from four other microturbulence simulation codes run at the same plasma operating point. Averaging over the time interval $t > 1000 L_T/v_{te}$, we find substantial agreement ($\pm 10\%$) between the GEM result, $\chi_{GEM} = 3.2$ $(\rho_e/L_T)\rho_e v_{te}$, and those from PG3EQ [$\chi_{PG3EQ} = 2.9$ $(\rho_e/L_T)\rho_e v_{te}$], GYRO [$\chi_{GYRO} = 2.9$ $(\rho_e/L_T)\rho_e v_{te}$], GENE [$\chi_{GENE} = 3.0$ $(\rho_e/L_T)\rho_e v_{te}$], and GS2 [$\chi_{GS2} = 2.4$ $(\rho_e/L_T)\rho_e v_{te}$]. The time-interval weighted average of the electron thermal conductivity over all of these simulation runs yields $\langle \chi_e \rangle \approx 3.0 \pm 0.13$ $(\rho_e/L_T)\rho_e v_{te}$. The GEM result is about 7% above this average thermal conductivity.

Having demonstrated that the heat transport in our GEM simulation is substantially the same as that of the PG3EQ, GYRO, GS2, and GENE simulations reported in Ref. 14 we turn our attention to the potential fluctuations responsible for this heat transport—in particular to the potential fluctuations at outboard midplane of these simulations. It is convenient to separate the potential at the outboard midplane into its toroidal average, $\langle \phi \rangle$ which we associate with zonal flows and geodesic-acoustic modes, and the deviations from this toroidal average, $\delta \phi \equiv (\phi - \langle \phi \rangle)$ which we associate with ETG turbulence. The potential fluctuation data from each simula-

tion should be viewed as a particular realization of an underlying turbulent ensemble. Our goal is to compare quantities characterizing the underlying turbulent ensemble of the potential fluctuations produced by each code. This underlying turbulent ensemble can be characterized by the fluctuation intensity, $I_{\delta\phi} \equiv \langle (\phi - \langle \phi \rangle)^2 \rangle$ and the two-point correlation functions, $C_{\delta\phi}$. In Fig. 2 the intensity of the ETG turbulence, $I_{\delta\phi}$, from our GEM simulation is compared to the intensity of the ETG turbulence reported in Ref. 14 from the PG3EQ, GYRO, and GS2 codes. At late times ($t > 1000 L_T/v_{te}$) the turbulent intensity from our GEM simulation is substantially the same as that observed in GYRO (the only other code for which we have a data set for the potential fluctuations of comparable length) where the late-time ($t > 1000 L_T/v_{te}$) average of the GYRO turbulent intensity is 22.3 $((\rho_e/L_T) \times (T/e))^2$ vs a late-time average turbulent intensity of 24.1 $((\rho_e/L_T)(T/e))^2$ from this GEM simulation. The lower value of the late-time fluctuation intensity from PG3EQ is attributed to the accumulation of discrete particle noise.[12,14] This is a larger issue for the PG3EQ run in question because it employed only 16 particles/grid-cell, while the GEM runs reported here employed 128 particles/grid-cell.

The correlation functions are also substantially the same [see Figs. 3(a) and 3(b)], allowing us to conclude that ETG potential fluctuations observed in this GEM simulation are
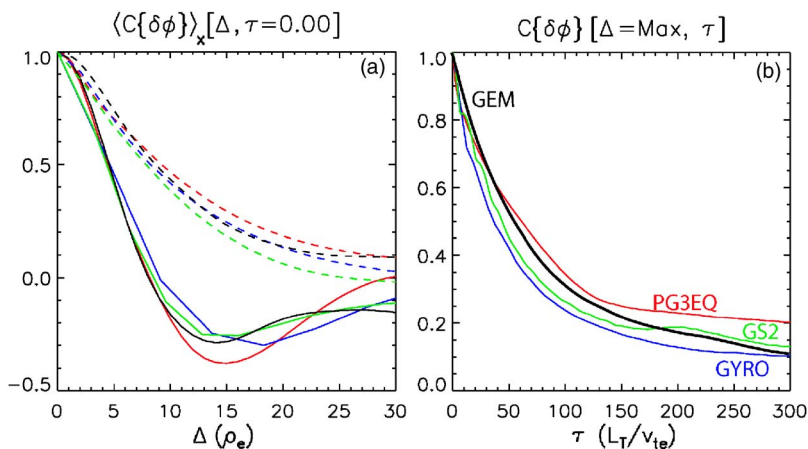

FIG. 3. (Color online) (a) The correlation function of the ETG turbulence at the outboard midplane is plotted vs the binormal separation (solid curves) and vs the radial separation (dashed curves). (b) The correlation function is plotted vs the time-lag. The GEM data are in black, PG3EQ in red, GYRO in blue, and GS2 in green.
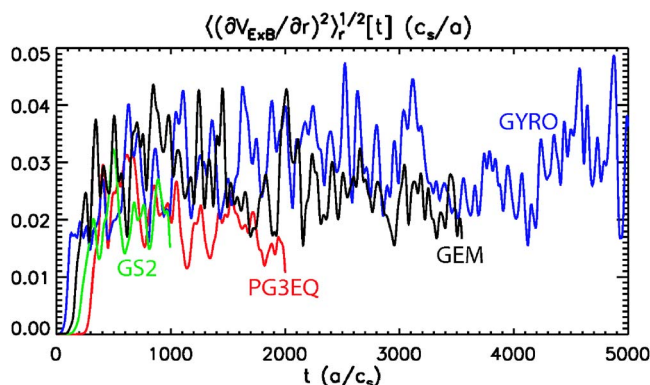
FIG. 4. (Color online) The rms $E \times B$ flow shear from GEM (black curve) is compared to the flow shear from PG3EQ (red curve), GYRO (blue curve), and GS2 (green curve).

substantially the same as those observed in the PG3EQ, GYRO, and GS2 simulations reported in Ref. 14.

It only remains to compare the toroidally averaged potential. Considerations of gauge and Galilean invariance imply that the $k_y = 0$ component of the potential affects the ETG turbulence mainly through the resulting $E \times B$ flow shear. The rms $E \times B$ flow shear from this GEM run is compared to those from PG3EQ, GYRO, and GS2 in Fig. 4. In making this comparison we have followed Ref. 14 in employing a digital filter to remove $k_y = 0$ fluctuations with radial wavelength less than the radial correlation length of the ETG turbulence ($10\rho_e$) and time scales less than the correlation time of the ETG turbulence ($100 L_T / v_{te}$). We see that the rms $E \times B$ flow shear is substantially the same in all of the runs. Comparing the late-time ($t > 1000 L_T / v_{te}$) average of the GEM and GYRO results, we find $\langle \partial V_{E \times B} / \partial r \rangle_{\mathrm{GEM}} \approx 0.025 v_{te} / L_T$, while $\langle \partial V_{E \times B} / \partial r \rangle_{\mathrm{GYRO}} \approx 0.030 v_{te} / L_T$.

In conclusion, benchmarking turbulence simulation codes is an important exercise in code verification. This code verification exercise is particularly important in light of recent controversies, in which particle and continuum codes showed qualitative differences in electron energy flux. In Ref. 14 four plasma microturbulence simulations codes were benchmarked—time did not allow inclusion of GEM data. Here, we correct the omission of GEM data in Ref. 14 and extend the results of that paper to include the GEM simulation code. We find that GEM agrees well with the other codes in the electron heat flux, the intensity and structure of the ETG turbulent fluctuations, and in the magnitude of the self-generated $E \times B$ flow shear.

In addition to the four-code ETG benchmark (here extended to five codes), Ref. 14 presented results from a scan over the magnetic shear, s, in which s was varied over the range $0.1 \leq s \leq 0.8$. Comparisons between GYRO simulations with adiabatic ions and full gyrokinetic ions demonstrated, for the parameters considered here, that the adiabatic ion approximation breaks down when $s > 0.4$. It was not possible to repeat these kinetic ion GYRO simulations using GEM because the ion Larmor radius is large compared to the perpendicular wavelength of the ETG turbulence. The GYRO simulations in question had a binormal resolution $k_{y,\mathrm{max}} \rho_e = 0.69$ and employed a mass ratio $m_i / m_e = 400$.

Hence, they required an accurate treatment of gyrokinetic ions out to $k_{y,\mathrm{max}} \rho_i \approx 14$ (which GYRO provides). The treatment of gyrokinetic ions involves gyroaveraging, which is complicated in particle-in-cell (PIC) codes, like GEM and PG3EQ, because it must be performed as part of the "gather/scatter" where information is interpolated between the continuous phase space of the computer particles and the discrete grid where the gyrokinetic Poisson equation is solved. At present, GEM, like PG3EQ and most other PIC codes, uses four points to approximate the gyroaverage, which provides a reasonable approximation to the gyroaverage provided that $k_{y,\mathrm{max}} \rho_i < 2$.[21] This is sufficient to resolve ion-scale turbulence (e.g., ion temperature gradient mode and/or trapped electron mode turbulence), but it would need to be upgraded to accurately resolve the kinetic ion response in ETG turbulence. We have performed GEM simulations with adiabatic ions at $s = 0.8$ and spatial resolution to $k_{y,\mathrm{max}} \rho_e = 0.81$. The result was similar to that reported for GS2 and PG3EQ at $s = 0.8$ in Ref. 14. The electron heat transport did not saturate. Instead both the heat flux and the turbulent intensity grew to very large values, resulting in an abnormal termination of this GEM run.

[1] F. Jenko, W. Dorland, M. Kotschenreuther, and B. N. Rogers, Phys. Plasmas **7**, 1904 (2000).

[2] W. Dorland, F. Jenko, M. Kotschenreuther, and B. N. Rogers, Phys. Rev. Lett. **85**, 5570 (2000).

[3] F. Jenko and W. Dorland, Phys. Rev. Lett. **89**, 225001 (2002).

[4] B. Labit and M. Ottaviani, Phys. Plasmas **10**, 126 (2003).

[5] Z. Lin, L. Chen, Y. Nishimura, H. Qu, T. S. Hahm, J. L. V. Lewandowski, G. Rewoldt, W. X. Wang, P. H. Diamond, C. Holland, F. Zonca, and Y. Li, *Fusion Energy 2004: Proceedings of the 20th Fusion Energy Conference, Vilamoura* (IAEA, Vienna, 2004), CD-ROM file TH8_4, see http://www-naweb.iaea.org/napc/physics/fec/fec2004/datasets/index.html

[6] Z. Lin, Bull. Am. Phys. Soc. **49**, 247 (2004), see http://www.aps.org/meet/DPP04/baps/index.html

[7] Y. Idomura, S. Tokuda, and Y. Kishimoto, *Fusion Energy 2004: Proceedings of the 20th Fusion Energy Conference, Vilamoura* (IAEA, Vienna, 2004), CD-ROM file TH/8-1, see http://www-naweb.iaea.org/napc/physics/fec/fec2004/datasets/index.html

[8] J. Li and Y. Kishimoto, Phys. Plasmas **11**, 1493 (2004).

[9] Z. Lin, L. Chen, and F. Zonca, Phys. Plasmas **12**, 056125 (2005).

[10] Y. Idomura, S. Tokuda, and Y. Kishimoto, Nucl. Fusion **45**, 1571 (2005).

[11] J. Q. Li, Y. Kishimoto, N. Miyato, T. Matsumoto, and J. Q. Dong, Nucl. Fusion **45**, 1293 (2005).

[12] W. M. Nevins, G. W. Hammett, A. M. Dimits, W. Dorland, and D. E. Shumaker, Phys. Plasmas **12**, 122305 (2005).

[13] S. Parker, J. Kohut, Y. Chen, Z. Lin, F. Hinton, and W. Lee, AIP Conf. Proc. **871**, 193 (2006).

[14] W. M. Nevins, J. Candy, S. Cowley, T. Dannert, A. Dimits, W. Dorland, C. Estrada-Mila, G. W. Hammett, F. Jenko, M. J. Pueschel, and D. E. Shumaker, Phys. Plasmas **13**, 122306 (2006).

[15] J. Candy and R. E. Waltz, J. Comput. Phys. **186**, 545 (2003).

[16] A. M. Dimits, T. J. Williams, J. A. Byers, and B. I. Cohen, Phys. Rev. Lett. **77**, 71 (1996).

[17] Y. Chen and S. Parker, J. Comput. Phys. **189**, 463 (2003).

[18] Y. Chen and S. Parker, J. Comput. Phys. **220**, 839 (2007).

[19] A. M. Dimits, G. Bateman, M. A. Beer, B. I. Cohen, W. Dorland, G. W. Hammett, C. Kim, J. E. Kinsey, M. Kotschenreuther, A. H. Kritz, L. L. Lao, J. Mandrekas, W. M. Nevins, S. E. Parker, A. J. Redd, D. E. Shumaker, R. Sydora, and J. Weiland, Phys. Plasmas **7**, 969 (2000).

[20] S. Parker, C. Kim, and Y. Chen, Phys. Plasmas **6**, 1709 (1999).

[21] W. W. Lee, J. Comput. Phys. **72**, 243 (1987).